



Multiplication of the depth of detectability using γ_{11n} arrays

Sándor Szalai^{a,*}, István Lempenger^a, Mohamed Metwaly^{b,c}, Árpád Kis^a, Viktor Weszttergom^a,
Kitti Szokoli^a, Attila Novák^a

^a RCAES HAS, GGI, H-9401 Sopron POB 5, Hungary

^b Archaeology Department, College of Tourism and Archaeology, King Saud University, Saudi Arabia

^c National Research Institute of Astronomy and Geophysics (NRIAG), Cairo, Egypt

ARTICLE INFO

Article history:

Received 21 August 2013

Accepted 4 June 2014

Available online 14 June 2014

Keywords:

Geoelectric array

Depth of investigation

Depth of detectability

ERT

γ_{11n} arrays

Parameter sensitivity

ABSTRACT

The depth from which one can get information has always been a crucial parameter in the geophysical exploration. This paper deals with the depth of detectability (DD) of 2D electric resistivity tomography configurations. DD is the maximal depth from which a given model body is detectable in the presence of a given noise level. Based on previous DD calculations for conventional electrode arrays it is shown in this paper that there is a nearly linear relation between the maximum value of their parameter-sensitivity (PS) maps and their DD values. Studying the PS maps of other arrays, as well, we found that many of them have higher PS_{max} values than those of the conventional arrays. These so-called γ_{11n} arrays are therefore expected to have larger DD values, too. The performed DD-calculations have confirmed this expectation. γ_{11n} arrays are linear geoelectric arrays where γ refers to the CPCP order of the current (C) and potential (P) electrodes whilst the subscript numbers refer to the distance of the neighbouring electrodes. In case of the studied prism and dyke models the γ_{11n} arrays – if n is larger or equal to 2 – consistently produced higher DD-values than the best conventional arrays. The DD value of these arrays can be even 2–3 times larger than that of the best conventional array value. Such an increase in the DD value is especially useful if the available place for measurements is limited, e.g. due to infrastructural conditions. Anomalies in large depth, for example, which are not seen by traditionally used arrays, may become detectable using γ_{11n} arrays as it was verified also by numerical studies. These arrays require moreover less measurement than most conventional arrays resulting in shorter measuring time.

© 2014 Elsevier B.V. All rights reserved.

1. Introduction

Depth of investigation (DI) is a basic parameter of all geophysical methods, including geoelectrics. The depth of investigation of geoelectric methods was at first attempted to be determined by Evjen (1938) by using the spatial distribution of the currents at depth. Later it became evident that the depth of investigation is inseparable from the selected array. Roy and Apparao (1971) defined depth of investigation of a given array as the depth, at which a thin-sheet produces maximum response. Roy (1972) and Bhattacharya and Dutta (1983) extended this approach to further arrays.

Alternatively, using the same Depth of Information Characteristic (DIC) function, Edwards (1977) recommended the use of the median depth, i.e. the depth at which the integral of the DIC function from the surface to the median depth is the same as from the median depth to infinity. Edwards (1977) found that this was in better agreement with his field experience. Szalai et al., (2009) have computed the parameter by

means of both the Roy and Apparao (1971) and the Edwards' (1977) approach for all 30 arrays it was reliable. As they have found that the median depth can be determined from the Roy–Apparao depth values by a multiplication with 1.59 ± 0.31 .

The foregoing DI calculations are however reliable only for nowadays rarely applied single arrays whilst they are not applicable for multi-electrode (ME) arrays. Moreover DI calculations haven't taken into consideration the effect of the noise. Ignoring the evidently present noise may lead to infinite DI values (Szalai et al., 2011). Szalai et al., (2011) introduced therefore the depth of detectability (DD) value providing a suitable parameter. DD is the maximal depth, where a given inhomogeneity can still be detected by means of a given ME-array, in the presence of a given level of noise. Studies based on the same principle, but using physical modelling have already been published by Apparao et al., (1992) and Apparao et al., (1997), but the results of these studies are less accurate due to the applied method.

Since we can't get any information of a certain inhomogeneity if we cannot detect it, we consider the foregoing definition as the basic parameter of the resistivity imaging method. Besides of that DD gives information about the limitations of the given ME array. In the study by Szalai et al., (2013) moreover arrays characterized by the highest DD values have the best imaging features.

* Corresponding author at: RCAES HAS, GGI, H-9401 Sopron POB 5, Hungary. Tel.: +36 99 508344; fax: +36 99 508355.

E-mail address: szalai@ggki.hu (S. Szalai).

Since the DD value is supposed to be therefore a basic quantity, it is crucial to find out if other arrays can produce higher DD values than the traditional arrays do. Apart from the ones that have been studied by Szalai et al., (2011) almost hundred other arrays have been applied before (Szalai and Szarka, 2008a).

Searching for such arrays we used parameter-sensitivity (PS) maps. A PS map is a map which shows the effect of an infinitely small volume element placed in a homogeneous half space and whose resistivity is different from that of the host. PS maps were first presented by Roy and Apparao (1971). Barker (1979) applied them to construct new arrays. Szalai and Szarka (2008b,c) presented PS maps for all ever used geoelectric arrays for which it is possible and demonstrated their potential.

In the present paper we demonstrate the way how we theoretically obtained specific ME-arrays which supposed to provide higher DD values than the conventional ones which were studied by Szalai et al., (2011). Computations of the DD values of these specific arrays have confirmed that certain ones have larger DD values than the conventional ones. This fact confirms the correctness of our theoretical approach and – in case of positive field test results – it may enable the utilization of these arrays in the geophysical practice. The perspectives of these arrays were strengthened by numerical studies, as well.

2. Method to calculate the DD values and the studied ME arrays

At first we introduce the method of calculation of DD (depth of detectability) and also recall the values formerly determined for conventional arrays.

The definition of the depth of detectability is illustrated in Fig. 1. The inhomogeneity in a given depth produces an apparent resistivity anomaly image which is calculated by forward modelling. The white/black

dotted line delineates the area where the relative anomaly is higher than 5 pc/10 pc that is the apparent resistivity values are less than 95 Ω m/90 Ω m contrary to the 100 Ω m background value. (For resistive models the apparent resistivity values should be more than 105 Ω m/110 Ω m, accordingly.) Increasing the depth of the model, the area encircled by the black/white dashed lines will be less and less. The depth at which the 10 pc black dashed lines disappear is called as depth of detectability with 10 pc noise (DD₁₀). At some larger depth, the 5 pc white dashed line will also disappear. Its depth is called as depth of detectability with 5 pc (DD₅). Below this depth the inhomogeneity cannot be detected in case of the given noise.

The DD values for prism and dyke models having both lower and higher resistivity than its environment were studied (Fig. 2). Due to the fact that nowadays the largest part of DC surveys is carried out by applying multielectrode systems and Loke's RES2DINV software (Loke, 1994, 1999), we applied the corresponding forward modelling code, RES2DMOD, version 3.0. The depth of the upper side of the model varied in the depth range of 0–14 m with a step of 0.5 m, in the depth range of 14–30 m with a step of 1 m, and it is increasing logarithmically below it to about 69 m (see the applied mesh on Fig. 1).

The parameters of the forward modelling are as follows: 100 electrodes were applied, and the electrode distance (the distance between the neighbouring electrodes) was 1 m. For the Wenner- α (W- α), Wenner- β (W- β), pole-pole (P-P) and dipole equatorial (DP-eq) arrays (Fig. 3a) 30 various electrode distances were applied; for the pole-dipole (P-DP) and dipole axial (DP-ax) arrays the dipole length was equal to the electrode distance and 50 different values for the distance between the dipoles were considered. These are the same arrays that have been studied in a former work by Szalai et al., (2011). In the present paper we completed the cited study with 10 further arrays, the γ_{11n}

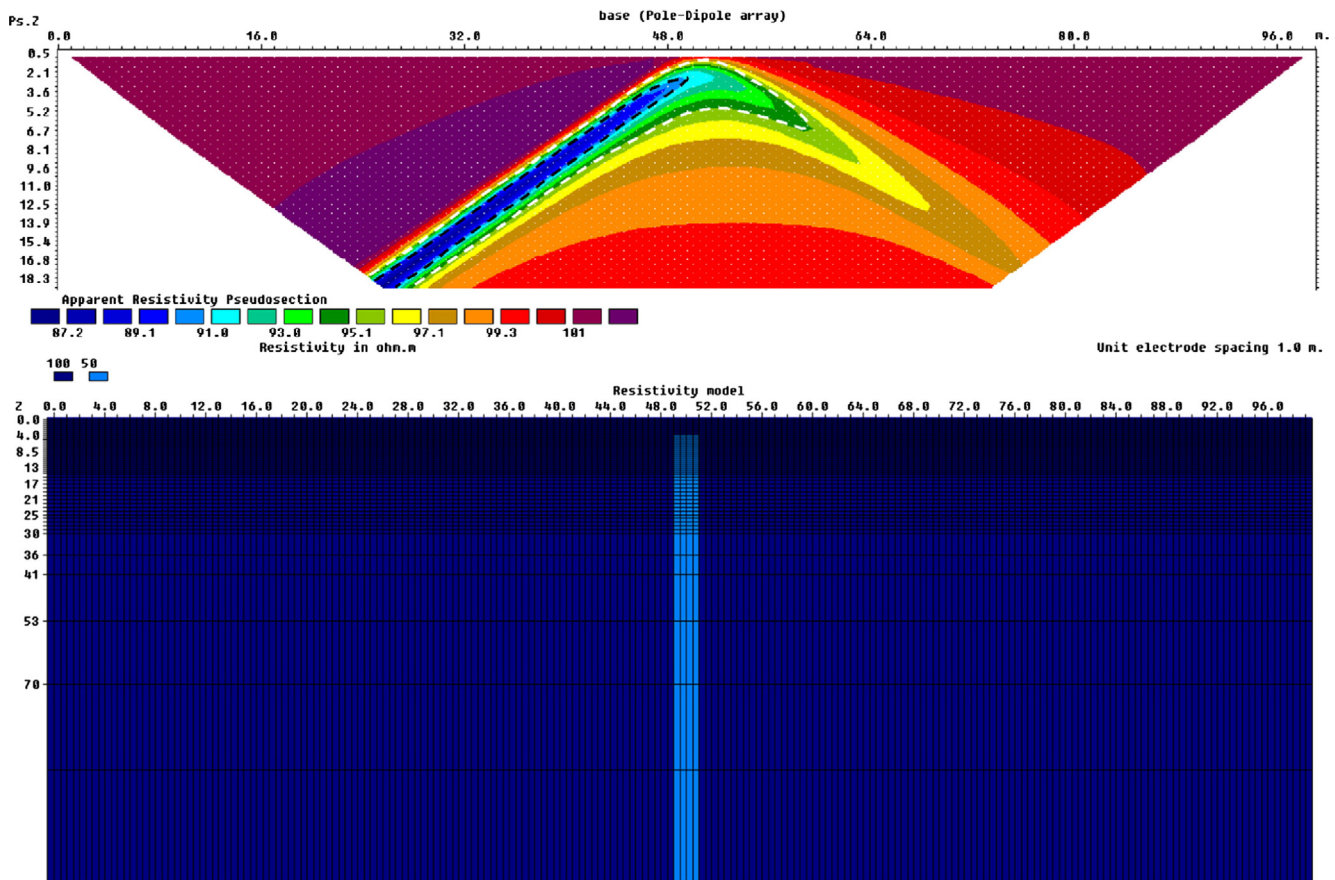


Fig. 1. A resistivity model and its response to illustrate the definition of the depth of detectability. The white/black dotted line delineates the area where the relative anomaly is higher than 5 pc/10 pc.

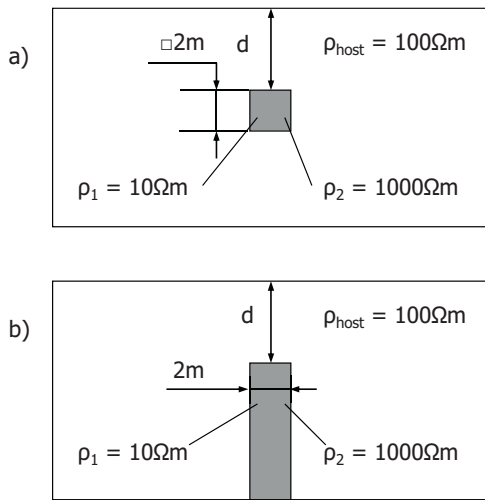


Fig. 2. The conductive and resistive variants of the applied models. a) Square prism; b) dyke.

($n = 1-6$), γ_{123} , γ_{124} , γ -quasi null and the Stummer arrays (Fig. 3b, c), which have been selected based on a consideration which is discussed in the 4-th chapter.

γ_{11n} represents a group of arrays (see Fig. 3c.). γ refers to the ranking of the electrodes, namely that the current and potential electrodes are installed in the so called overlapping mode, having one potential electrode between the current electrodes. The parameters in '11n' refer to the distance between the neighbouring electrodes of the given array, where '1' is the unit distance, the distance between the neighbouring electrodes in ME systems. The γ_{123} - and γ_{124} -arrays (Fig. 3c) are also members of this series.

Whilst in case of the classic γ -null array (Szalai et al., 2004) the distance of the inner electrodes would be approximately 62% of the distance of the first/last two electrodes it is only 50% for the γ -quasi null array (Fig. 3b). Since the potential difference measured by this array above homogeneous half space is not zero, but relatively small, such arrays are referred as quasi null arrays.

As recently we are facing with increasing demand of optimised ERT-measurements (Stummer et al., 2004; Wilkinson et al., 2006), we also have extended our study with an optimised array, the so-called Stummer array (Stummer et al., 2004). This is a model independent configuration whose electrode installation can be found in the Appendix of the cited paper. Whilst the configuration is given for only 30 electrodes the electrode distance of the Stummer array was increased to have a section length comparable to the other studied arrays. In spite of a similar modification the Stummer array proved to be the best array in numerical studies (Szalai et al., 2013).

The data points for each arrays were as follows: W- α : 1605; W- β : 1605; P-P: 2535; P-DP: 3675; DP-eq: 2535; DP-ax: 3625; St: 669; γ_{111} : 1617; γ_{112} : 1200; γ_{113} : 950; γ_{114} : 784; γ_{115} : 665; γ_{116} : 576; γ_{123} : 784; γ_{124} : 665; and γ -null: 1200. γ_{11n} ME-arrays, if $n \geq 2$, have less data points than the conventional ME arrays which result a faster field measurement.

3. Results for the traditional arrays

The results of the traditional arrays excluding those of the Stummer array (Table 2a) are taken from Szalai et al., (2011). The depth of detectability values depend strongly on the models. If inhomogeneities have small lateral extension (like the presented prism and dyke models), the P-DP and DP-ax arrays proved to be the best ones. The worst results, with one single exception, were obtained by using the P-P and W- α

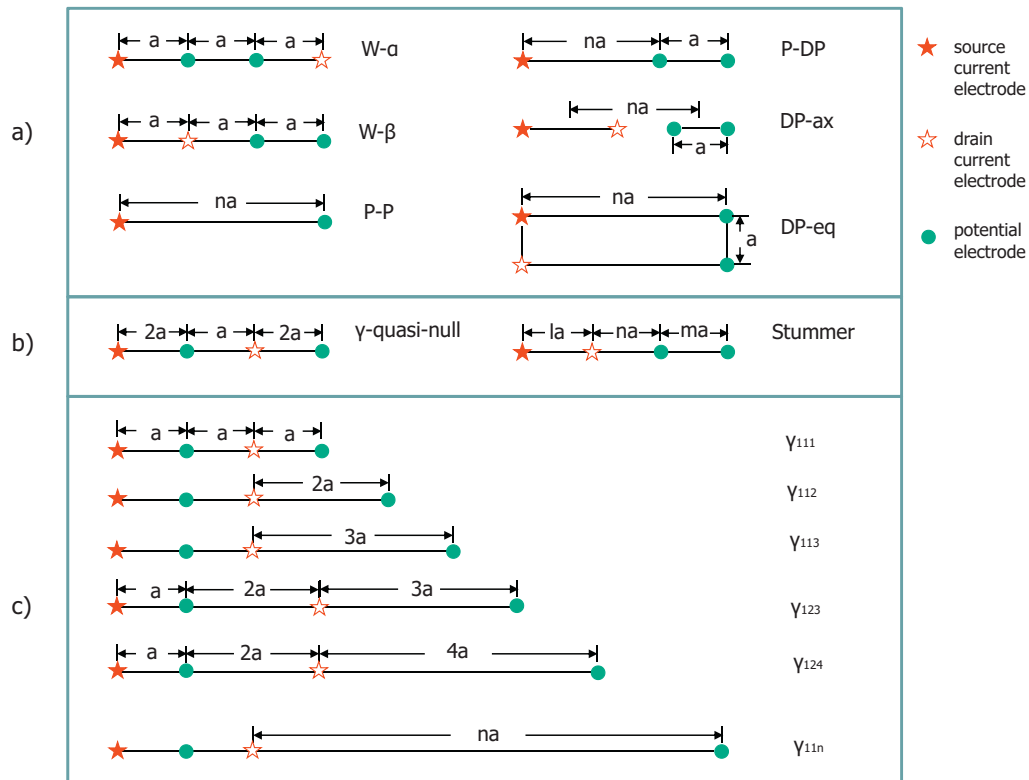


Fig. 3. a) Arrays investigated by Szalai et al., (2011). b) and c) The in this paper investigated arrays. In case of $n = \infty$, the γ_{11n} array turns into the MAN array. Stars denote current electrodes, circles denote potential electrodes.

arrays. In case of these inhomogeneities the W- β and DP-eq arrays proved to be neither the best nor the worst arrays (Szalai et al., 2011).

The DD values of various geoelectric arrays for a given model cover a wide range: there can be even a ratio of 3–4 between the maximum and minimum values. Other arrays might provide higher DD-values therefore we studied the relation of DD and PS map maximums.

4. Searching for arrays having higher DD values

It looks logical that there is a formal relation between the maximum value of the parameter-sensitivity (PS) map and the DD-value (depth of detectability) of an array. Szalai and Szarka (2000) have namely demonstrated that the maps received using realistic size cubes are similar to the PS maps. Due to that a 3D volume element below the line of the array produces (in case of collinear arrays) the largest part of the effect of a 2D prism having the same cross-section a relation between the PS_{\max} and prism DD values can be expected. The dyke DD is expected to give the same relation, because the dyke's main contribution to the signal originates from its uppermost part.

Therefore we have studied the PS_{\max} value of the arrays seen in Figs. 4 and 5 which was analysed by Szalai and Szarka (2008b,c). The PS_{\max} ranking of the arrays with the related PS_{\max} values in $z/R = 0.1$ depth is as follows: 1. DP-eq: 9, 2. DP-ax: 7, 3. P-DP: 6.5, 4. W- β : 4, 5. W- α : 2.2, 6. PP: 0.18 (Table 1). (Note that the ranking of the arrays which bases on the PS_{\max} values slightly changes with increasing depth as it is seen in Figs. 4 and 5, but because the signal predominantly originates from shallow depth we considered the PS_{\max} value in $z/R =$

0.1 depth decisive, where R is the array length.) The “goodness” ranking was the same in the DD investigations (Szalai et al., 2011) which means that an array with larger PS_{\max} value has also higher DD value.

The only exception is the DP-eq array, whose DD value is significantly lower than expected. It has a simple explanation: this array is predominantly sensible for the y component (value: 8.5), the dipole momentum of the small volume element perpendicular to the connecting line of the dipoles (Fig. 6), whilst the influence of the x component – which is important in 2D ERT – is relatively weak, 1.1.

Regarding the relation between the PS_{\max} and DD values it seemed to be worthwhile to see whether there are arrays having larger PS_{\max} values than the traditional arrays. Thus we listed the PS_{\max} values (Table 1) of all arrays studied by Szalai and Szarka (2008b,c). Noteworthy is the extremely high value of the qMAN (gtt) array. It is a γ_{11n} array (similar to the ones in Fig. 3c, but $n = 8$), a modified version of the MAN array (γ_{11n} array, $n = \infty$, Szalai et al., 2004). It can be implemented in ERT systems without dealing with electrode installed in the infinity but it would result too few measurement points due to the large length of the array. It is therefore subservient to make a compromise between the length of the array and the expected PS_{\max} . We suppose that the PS_{\max} value of the γ_{11n} arrays decreases with decreasing n . To achieve sufficient number of data it is subservient to decrease n , the distance of the last two electrodes to 4–5 times the electrode distance. The γ_{114} , and γ_{115} -arrays (see Fig. 3c, $n = 4.5$) were therefore taken into account. But the DD values of the γ_{111} , γ_{112} , γ_{113} and γ_{116} -arrays were also studied to have an overview about the γ_{11n} arrays.

It looked possible that also the γ_{123} and γ_{124} arrays, which are similar to the γ_{11n} ones, can have large DD values. Therefore their DD values

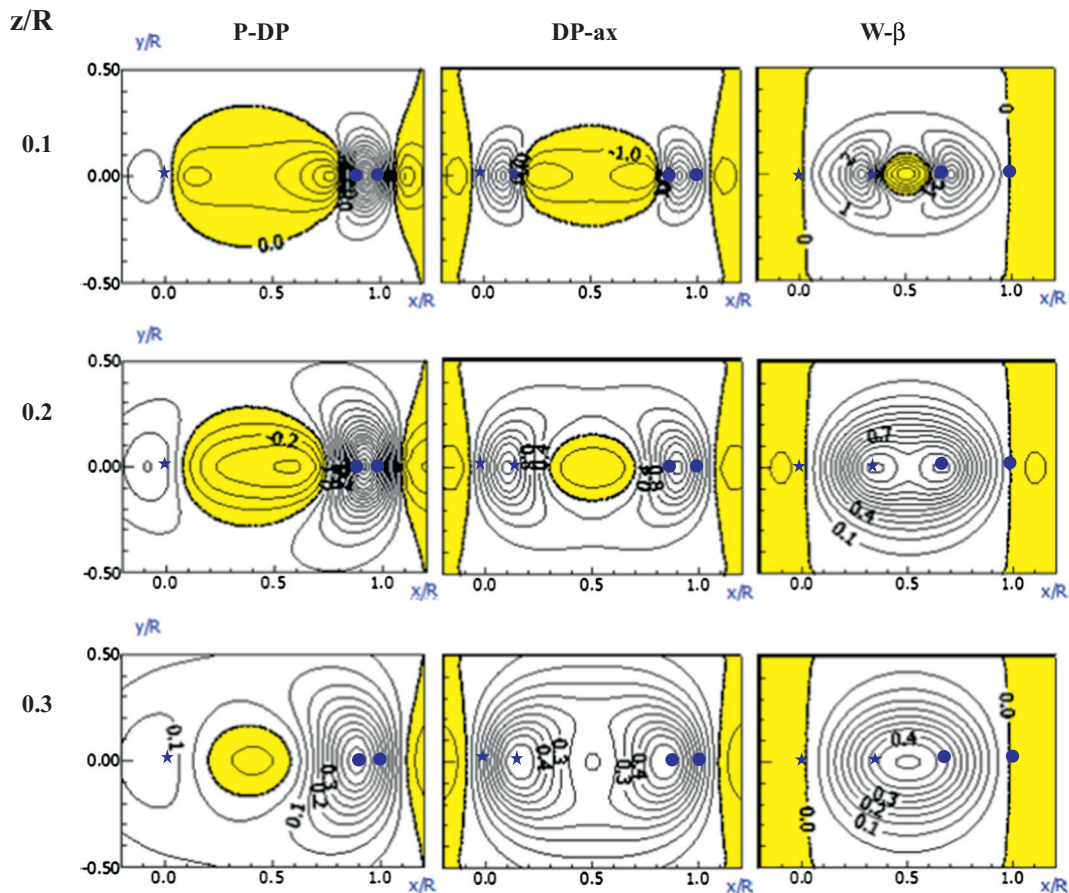


Fig. 4. PS maps of DC arrays studied by Szalai et al., (2011): pole-dipole (P-DP), dipole axial (DP-ax) and Wenner- β (W- β) arrays at 3 different z/R depth levels (R : array length). Stars denote current electrodes, circles denote potential electrodes. Thick black line indicates the zero level. In the yellow areas the values are negative. The distance of the contour lines is for the P-DP array at $z/R = 0.1, 0.2$ and 0.3 depths: 0.5, 0.1 and 0.05, accordingly. For the DP-ax array: 1, 0.2 and 0.05. For the W- β array: 0.5, 0.1 and 0.05. (For interpretation of the references to colour in this figure legend, the reader is referred to the web version of this article).

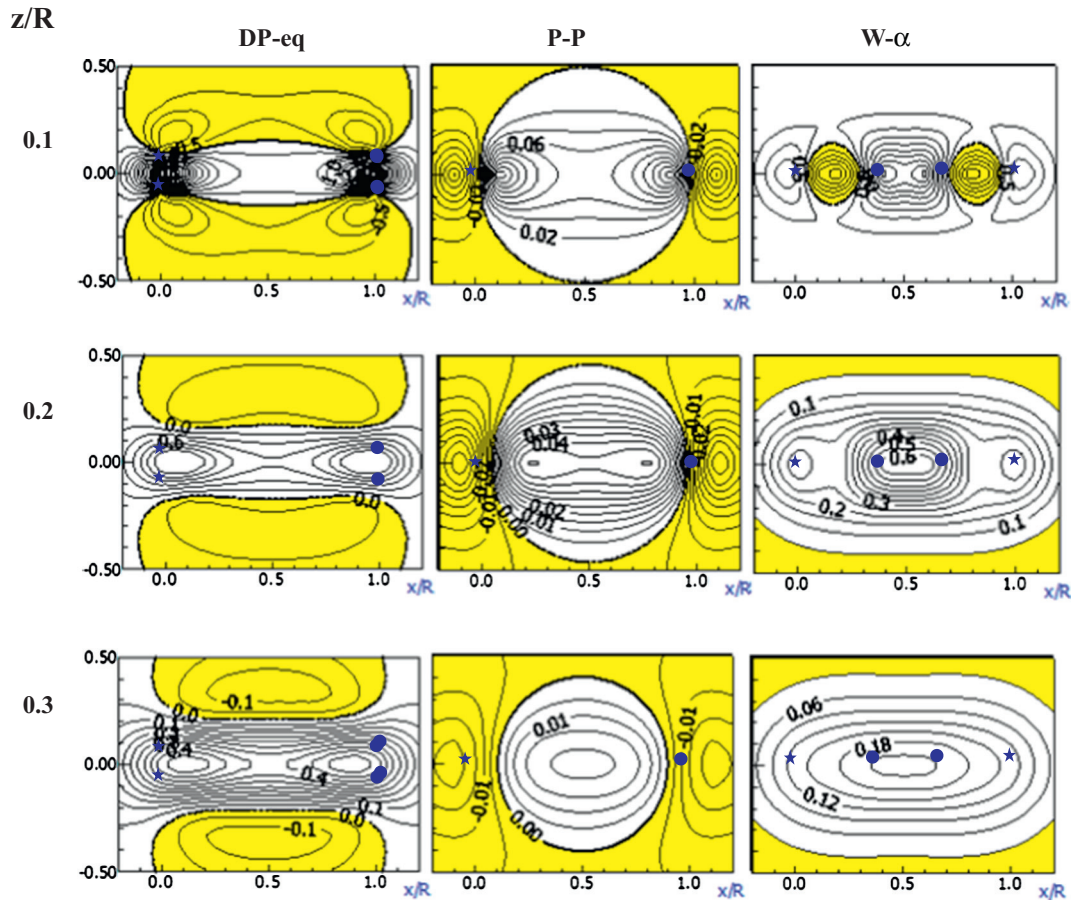


Fig. 5. PS maps of DC arrays studied by Szalai et al., (2011): dipole equatorial (DP-eq), pole-pole (P-P) and Wenner- α (W- α) arrays at 3 different z/R depth levels (R : array length). Stars denote current electrodes, circles denote potential electrodes. Thick black line indicates the zero level. In the yellow areas the values are negative. The distance of the contour lines is for the DP-eq array at $z/R = 0.1, 0.2$ and 0.3 depths: 0.5, 0.25 and 0.05, accordingly. For the P-P array: 0.02, 0.005 and 0.005. For the W- α array: 0.25, 0.05 and 0.03.

Table 1

The arrays studied in Szalai and Szarka (2008b,c) are ranked in accordance with the related PS_{max} . For the figure of the given arrays see Szalai and Szarka (2008b, c), for their origin see Szalai and Szarka (2008a). The italicized items are nonlinear or focussed geometries. The bold typed arrays are the ones studied in Szalai et al., (2011).

Array name	PS_{max} value
qMAN (gtd)	120.0
Dipole equatorial (DP90)	9.0
Schlumberger	8.0
a0304	7.0
Dipole axial	7.0
Unipole- β	7.0
Pole-dipole (half-Schlumberger)	6.5
ght (half-Twin)	5.5
Dipole parallel 54°	5.0
a0105	5.0
Wenner-β	4.0
Wenner- γ	4.0
Unipole- γ	3.3
gt (Twin)	2.8
Dipole axial null	2.7
a0103	2.4
Wenner-α	2.2
Square- γ	2.0
Three-electrode null (nhs)	1.8
Half-Wenner (ahW)	1.8
Schlumberger null (ns)	1.4
Square- α (sa)	1.0
Unipole- α	0.8
Pole-pole (b2el)	0.18

were determined, as well. The γ -quasi-null array (Fig. 3b) was also investigated because its homogeneous half space value is close to zero. We wanted to see how this feature influences the DD value of an array.

Hereafter we determine the DD value of all these arrays and compare them with the DD values of conventional arrays.

5. DD results for all arrays

Figs. 7 and 8 present the $100|\rho_{ext}-\rho_1|/\rho_1$ value for both the prism and dyke models both the conductive and resistive ones. These figures served as a basis to determine the DD values of the given arrays. The depth where they reach 5/10 pc is their DD (depth of detectability) value for the given noise level.

In Table 2 the DD values of both the former studied and the only in this paper investigated arrays are summarised. In some cells however no values are displayed. It is for one of the following reasons:

- 1) The signal was below the noise level on the whole section (conductive dyke, 10% noise, W- α and γ_{111} arrays; both dykes, 10 pc noise, γ -q-null array). It means that the model is undetectable besides the given noise level.
- 2) In certain cases the DD values are even larger than the studied 25 m depth (all other unloaded cells, e.g. for resistive dyke, γ_{114} array, 5 pc noise).

As mentioned before amongst the conventional arrays the P-DP and DP-ax arrays have the highest DD values. The only exception is the

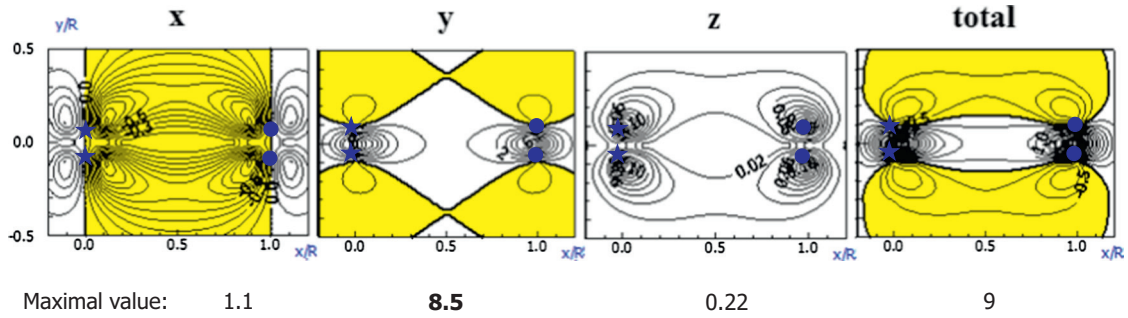


Fig. 6. PS maps of the equatorial dipole array. The PS maps for the side pairs perpendicular to the given axis and for the whole model body. Stars denote current electrodes, circles denote potential electrodes. All maps are made for $z/R = 0.1$ depth.

conductive prism model, where the DP-eq was the most efficient for both 5 pc and 10 pc noise.

The DD values of the γ_{11n} ($n = 1, 6$) arrays systematically increase with increasing n in case of the studied models. Whilst the DD value of the γ_{111} array doesn't exceed the DD values of the best conventional array for any model, the γ_{11n} arrays, if $n \geq 2$ provide higher DD values than the conventional arrays for each model (Table 2).

The DD values of the γ_{123} , and the γ_{124} -arrays are however not larger than those of the best conventional arrays. The γ -quasi-null array provides even smaller DD values, which verifies, that just to have small homogeneous half space signal is not enough to produce large DD value.

The Stummer array provided similar values as the DP-ax array. It is although expected since about the first 600 term of the Stummer array is bipole–bipole type, similarly to the DP-ax array (Stummer et al., 2004). The imaging capacity of the DP-ax and the Stummer arrays is also similar (Szalai et al., 2013).

Fig. 9 demonstrates for example that assuming 5% noise level only the γ_{11n} arrays ($n = 3–6$) can detect the conductive prism which is in 8 m depth. Only the pseudosections of these arrays have values less than 95 Ω m which are denoted by the thick white lines. In Fig. 9 the ranking of the arrays is the same as their DD ranking for conductive prisms.

Summarising the aforesaid results the γ_{11n} arrays provide the largest DD values as it was expected. These investigations also verified that the PS map is suitable – amongst many other possibilities (Szalai and Szarka, 2008b) – for estimating the related DD. The larger the PS map maximal value the larger is the DD.

Besides the larger DD values of the γ_{11n} arrays there are still several other motivations to study them. These items will be summarised in the next chapter.

6. Motivations to study the γ_{11n} arrays

- As it has been previously shown the γ_{11n} ME-arrays provide higher DD-values than other investigated arrays. It may have a great importance also since arrays having higher DD-values seem to have better imaging characteristics (Szalai et al., 2013).
- It has already been demonstrated that null-arrays can be effective and practical for field measurements, too (Falco et al., 2012; Szalai et al., 2002). There is however only one null array, the MAN array which is feasible to build in 2D ME-systems (Szalai et al., 2004). The inversion of the MAN data is however not resolved yet by the worldwide used softwares (Res2DInv, EarthImager). Therefore it is of great importance to perform a detailed analysis of the γ_{11n} arrays, which are very similar to the MAN array (see Fig. 3.) and whose data can be inverted if even with limitations.
- We suppose that the so called quasi null arrays like the γ_{11n} arrays – which represent a kind of transition between the null arrays and the conventional arrays – might provide better imaging characteristics than the null arrays in certain circumstances.
- Stummer et al., (2004) haven't included the γ -type arrays (they called them Wenner- γ arrays) in the optimisation procedure. If however these arrays provide to be useful they have to be taken into account in the optimisation process to get the really “best” configuration.

The γ_{11n} arrays seem to be therefore very worthwhile for further investigation. A number of numerical examples are presented in Szalai et al., (2014). Here just some examples will be shown to validate their suitability.

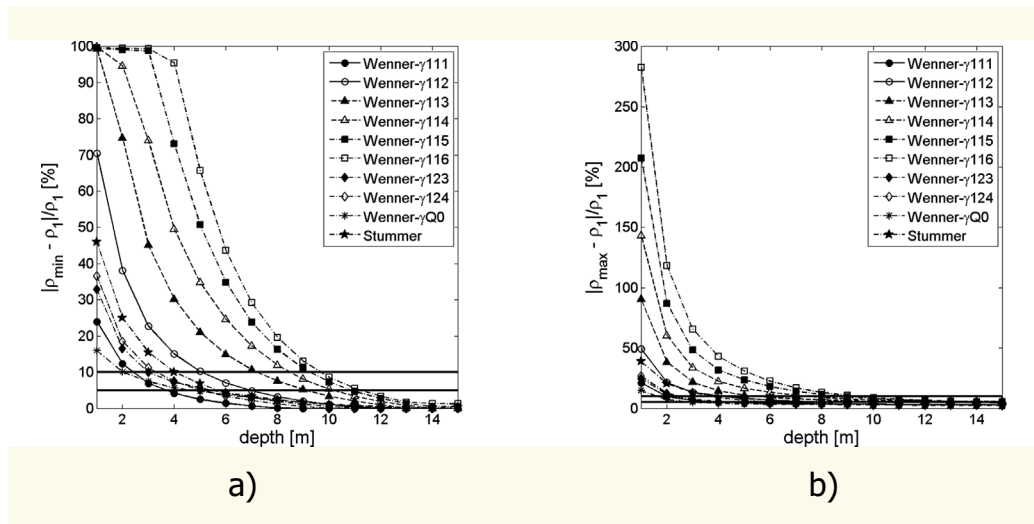


Fig. 7. The $100|\rho_{\text{ext}}-\rho_1|/\rho_1$ values for the investigated DC arrays and for the square prism model, as a function of the depth of the top of the target. (a) Conductive prism, (b) resistive prism.

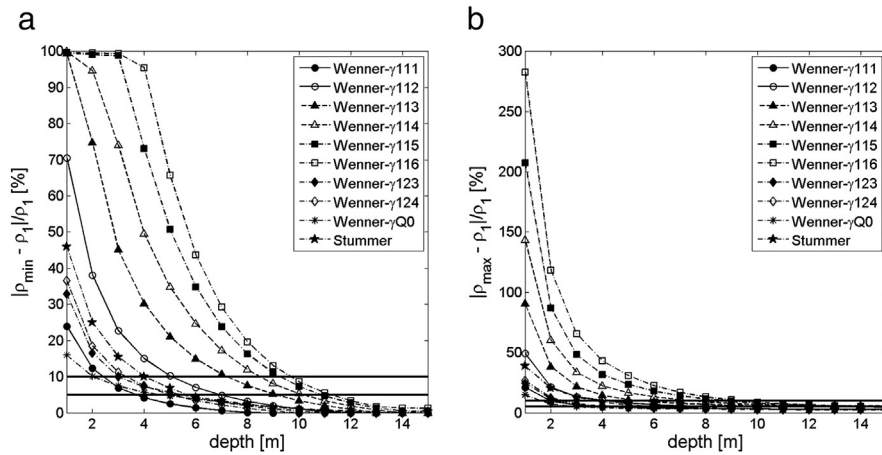


Fig. 8. The $100|\rho_{\text{ext}} - \rho_1|/\rho_1$ values for the investigated DC arrays and for the dyke model, as a function of the depth of the top of the target. (a) Conductive dyke, (b) resistive dyke.

7. Numerical modelling

Demonstrating the suitability of the γ_{11n} arrays we have performed numerical modelling. EarthImager 2D version 2.1.6 has been used for modelling. Finite Element Method was applied for the forward modelling and robust inversion for the inversion. All settings are the same like in Szalai et al., (2013). Here we note only the settings different from the default ones: Minimum apparent resistivity was taken to $-10000 \Omega \text{ m}$ (negative values may occur), Vertical/Horizontal Roughness Ratio to 5, the estimated noise of resistivity data to 2pc, the Initial Damping Factor to 0.01. 5 pc Gaussian noise was added to the calculated data prior to the inversion to get Figs. 10–12. Note that the RMS values are less than 6 pc for all arrays and models.

The numerical modelling verified that certain γ_{11n} arrays are really able to display model bodies which are not seen by other arrays. In Fig. 10, e.g. the inverted resistivity sections for a conductive prism model in 8 m depth can be seen. The sections are arranged according to their DD (depth of detectability) values for the conductive prism model. It is well seen that the prism is correctly displayed only on the γ_{11n} ($n = 3-6$) images. These arrays were those which produced the highest DD values for this type of model. These sections show the anomaly at correct

position and without any significant artefacts in contrary to the other arrays.

Fig. 11 presents the inverted resistivity sections for a model consisting of three conductive prisms in 8 m depth. The images are acceptable beginning from the Stummer array's image. The following arrays could detect the prisms and they were more or less able to separate them from each other. Regarding the separation, the γ_{112} , the Stummer and particularly the γ_{115} arrays proved to be the best ones.

Fig. 12 illustrates the inverted resistivity sections for a model consisting of three conductive dykes in 8 m depth. In this case the γ_{115} and γ_{116} arrays produced by far the best results that are those ones which have the largest DD value for conductive dykes.

The presented numerical examples confirmed therefore the usefulness of the in this paper presented investigations. They also verify that arrays having larger DD values may give better inverted image.

8. Conclusions

The DD (depth of detectability) values of different geoelectric multi-electrode configurations have been studied in this paper. It is a crucial parameter because it describes the limits of an array and gives a

Table 2

5 pc and 10 pc DD (depth of detectability) of the investigated arrays in metres for the two (resistive and conductive) variants of the two models, shown in Fig. 2.

a) DD values of the conventional arrays: the ones investigated by Szalai et al., (2011) and the Stummer array. The arrays which provide the highest DD for a given model and noise level are set with bold type fonts.

b) DD values of the γ arrays. The smallest DD value which exceeds the maximum DD of a), are set with bold type fonts).

Noise	Square prism conductive (1)		Square prism resistive (2)		Dyke conductive (3)		Dyke resistive (4)	
	5%	10%	5%	10%	5%	10%	5%	10%
a)								
W-α	2.65	1.84	3.8	2.03	1.53	–	4.77	1.48
W-β	5.61	3.8	5.47	3.1	3.43	1.73	4.84	1.98
P-P	4.2	2.72	3.73	2.08	2.44	1.2	3.04	1.27
P-DP	5.37	3.67	6.62	3.9	4.03	2.44	8.63	4.43
DP-eq	6.27	4.28	4.28	2.13	2.72	1.48	4.25	1.39
DP-ax	5.91	4.05	6.6	3.9	4.13	2.47	8.56	4.45
St	5.67	4.01	6.3	3.7	3.71	2.23	7.51	3.73
b)								
γ111	3.65	2.33	4.4	1.97	1.8	–	6.74	1.76
γ112	6.93	5.1	8.64	4.13	5.4	3.18	25	5.05
γ113	9.1	7.2	14	5.42	7.98	5.72	–	5.9
γ114	10.15	8.46	–	7.47	9.1	7.13	–	7.11
γ115	10.86	9.25	–	8.71	9.84	8	–	8.25
γ116	11.23	9.64	–	9.31	10.23	8.42	–	8.82
γ123	5.46	3	4.2	2.23	2.94	1.3	4.76	1.49
γ124	5.04	3.28	4.45	2.36	3.36	1.61	4.47	1.62
γ-q-n	4.7	2.03	3.03	1.5	3.1	–	3.77	–

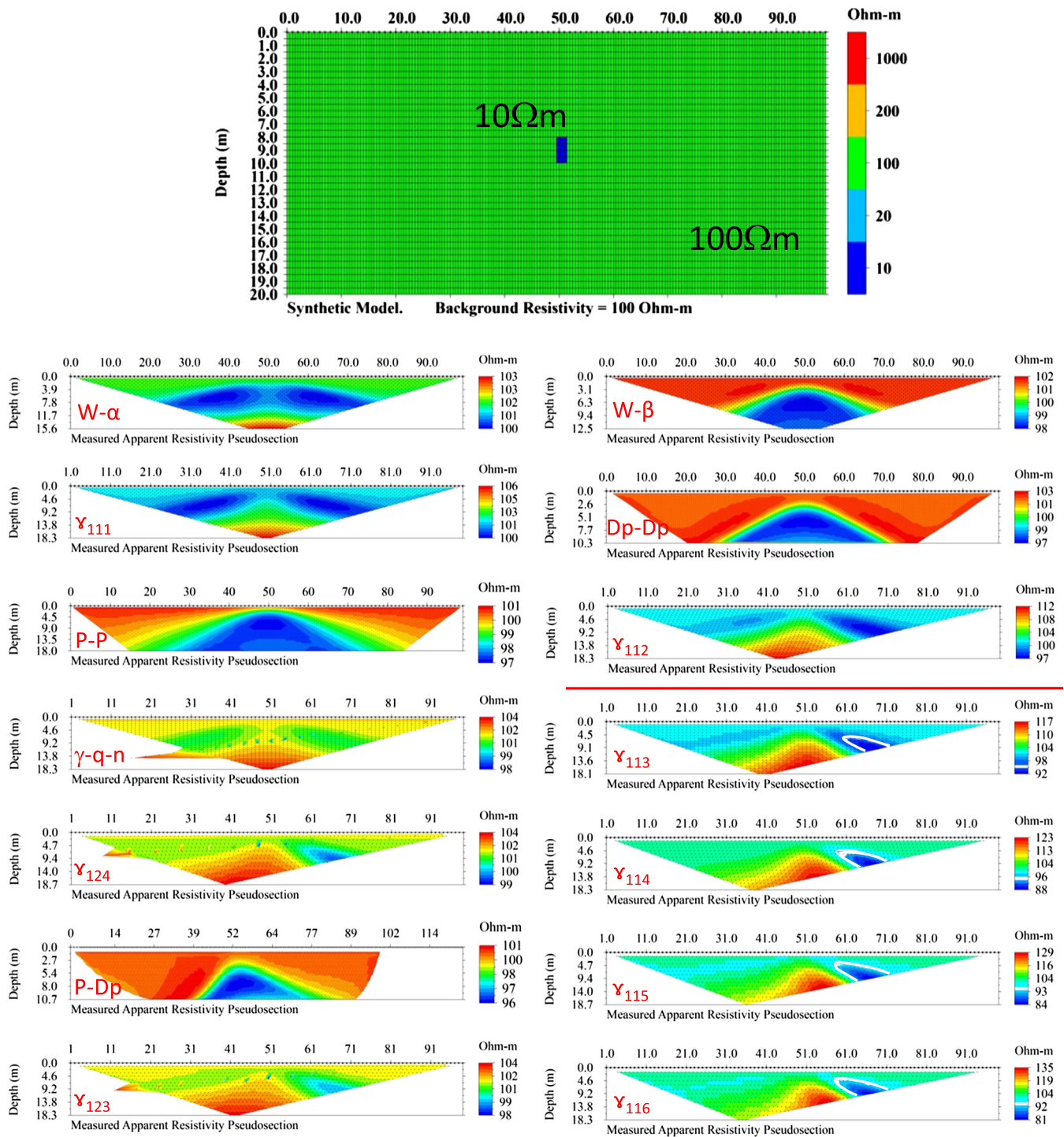


Fig. 9. Calculated apparent resistivity sections for the investigated arrays to demonstrate the DD definition. Depth of the prism is 8 m. Assumed noise level is 5%. The thick white line encircles areas where the resistivity value is less than 95 Ω m.

prediction about its imaging capacity. On the basis of the relation between the DD and the PS_{max} values of the geoelectric arrays we found certain arrays which have larger DD value than the traditional arrays. Our results in details:

1. Based on the results of previously conducted DD calculations for conventional arrays we demonstrated the relation between their PS map maximums and DD values.
2. Over viewing the PS maps of all arrays it was found that certain arrays provide higher PS_{max} values than the conventional ones. Therefore

these arrays are expected to have larger DD value. The DD values of these arrays were calculated and they verified this expectation.

3. The DD values of 10 arrays have been calculated for the first time.
4. Both for prism and dyke models either more or less resistive than the background the γ_{11n} arrays (for $n \geq 2$) consistently provided larger DD values than the best conventional arrays, the pole-dipole and axial dipole ones. The DD values of the γ_{11n} arrays can be even 2–3 times higher than those of the best conventional arrays. At the same time the γ -quasi null array and even the optimized Stummer array provide only moderately good DD value;

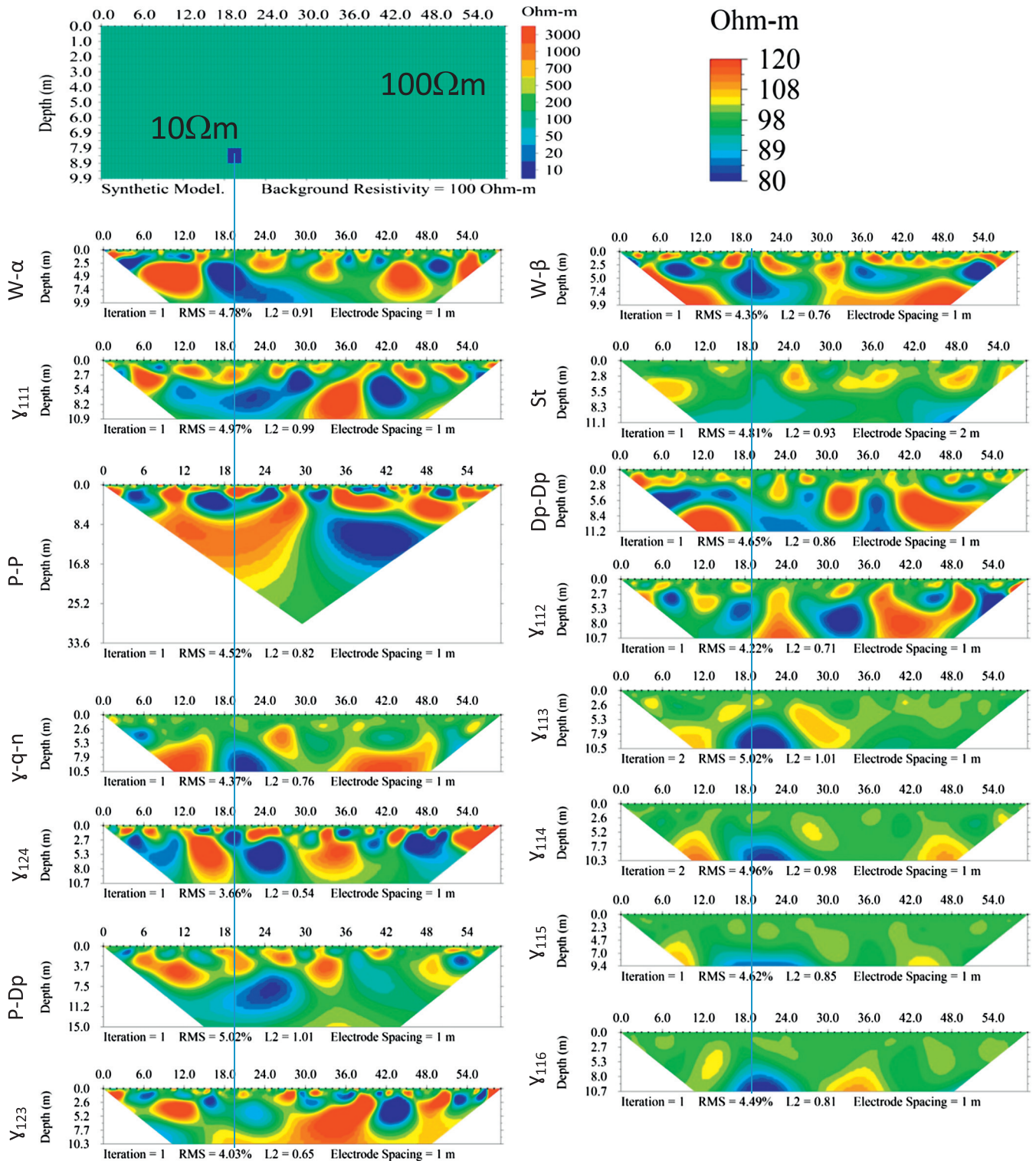


Fig. 10. The inverted resistivity sections for a conductive prism model in 8 m depth assuming 5% noise level. The sections are arranged according to their DD values for the conductive prism model.

5. The DD value of the γ_{11n} arrays is moreover larger than that of the conventional arrays in spite of that it requires less than half of the number of measurements than the W-α or W-β arrays and less than 25 pc of measurement that is required for the P-DP and DP-ax arrays.
6. The applicability of the γ_{11n} arrays was verified by numerical investigations. These arrays produced better inverted sections than the

- conventional arrays. Especially the γ_{115} and γ_{116} arrays which proved to be very effective in spite of their rather limited data.
7. Based on the inversion results the quality of the inverted image seems to be more related to the DD value of an array than to its data number.

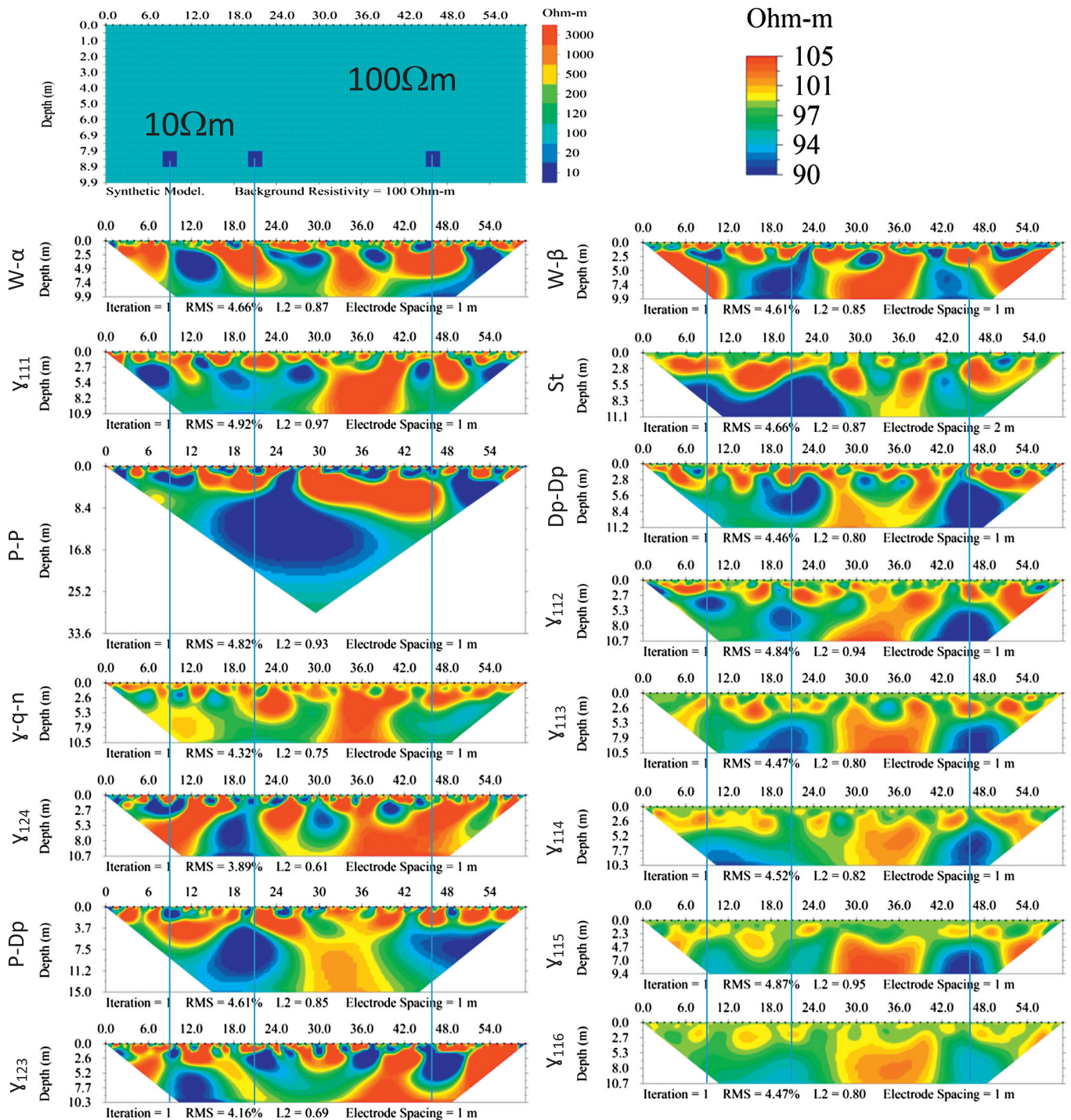


Fig. 11. The inverted resistivity sections for a model consisting of three conductive prisms in 8 m depth assuming 5% noise level. The sections are arranged according to their DD values for the conductive prism model.

According to the above observations the γ_{11n} arrays and particularly the γ_{112} , γ_{113} and γ_{114} ones can be useful alternatives of the conventional arrays particularly in sites where the place available for measurements is limited (e.g. built up areas), because they are able to give information from larger depth. Measurements with these arrays are moreover less time consuming.

Acknowledgement

Hungarian National Research Fund, project number K49604. S. Szalai, one of the authors of this paper is a grantee of the Bolyai János Scholarship.

References

- Apparao, A., Gangadhara Rao, T., Sivarama Sastry, R., Subrahmanya Sarma, V., 1992. Depth of detection of buried conductive targets with different electrode arrays in resistivity prospecting. *Geophys. Prospect.* 40 (7), 749–760.
- Apparao, A., Sivarama Sastry, R., Subrahmanya Sarma, V., 1997. Depth of detection of buried resistive targets with some electrode arrays in electrical prospecting. *Geophys. Prospect.* 45 (3), 365–375.
- Barker, R.D., 1979. Signal contribution sections and their use in resistivity studies. *Geophys. J. R. Astron. Soc.* 39, 123–129.
- Bhattacharya, B.B., Dutta, I., 1983. Depth of investigation studies for gradient arrays over homogeneous isotropic half space. *Geophysics* 48, 1248–1251.
- Edwards, L.S., 1977. A modified pseudosection for resistivity and IP. *Geophysics* 42, 1020–1036.

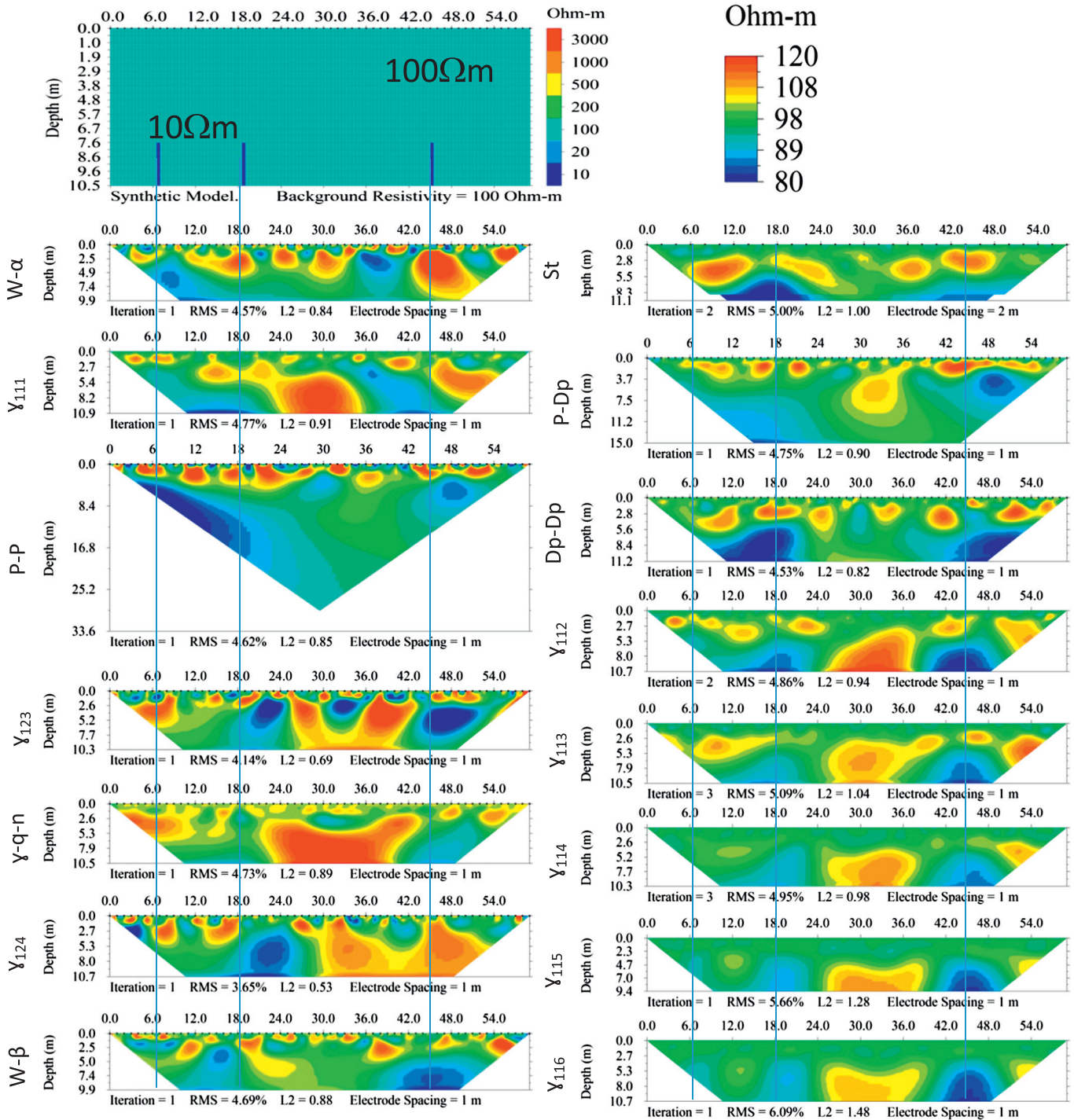


Fig. 12. The inverted resistivity sections for a model consisting of three conductive dykes in 8 m depth assuming 5% noise level. The sections are arranged according to their DD values for the conductive dyke model.

Evjen, H.M., 1938. Depth factors and resolving power of electrical measurements. *Geophysics* 3, 78–95.

Falco, P., Negro, F., Szalai, S., Milnes, E., 2012. Fracture characterisation using geoelectric null-arrays. *J. Appl. Geophys.* 93, 33–42.

Loke, M.H., 1994. The inversion of two-dimensional apparent resistivity data. *Unpubl. Ph. D. thesis*, University of Birmingham (U.K.).

Loke, M.H., 1999. RES2DMOD ver. 2.2. Rapid 2D resistivity forward modelling using the finite difference and finite-element methods. Wenner (alpha, beta, gamma), inline & equatorial dipole-dipole, pole-pole, pole-dipole and Wenner-Schlumberger. Freeware Courtesy of M. H. Loke, (available from www.geoelectrical.com).

Roy, A., 1972. Depth of investigation in Wenner, three electrode and dipole-dipole dc resistivity methods. *Geophys. Prospect.* 20, 329–340.

Roy, A., Apparao, A., 1971. Depth of investigation in direct current methods. *Geophysics* 36, 943–959.

Stummer, P., Maurer, H., Green, A.G., 2004. Experimental design: electrical resistivity data sets that provide optimum subsurface information. *Geophysics* 69 (1), 120–139. <http://dx.doi.org/10.1190/1.1649381>.

Szalai, S., Szarka, L., 2000. An approximate analytical approach for computing geoelectric response due to a small buried cube. *Geophys. Prospect.* 48, 871–885.

Szalai, S., Szarka, L., 2008a. On the classification of surface geoelectric arrays. *Geophys. Prospect.* 56, 159–175. <http://dx.doi.org/10.1111/j.1365-2478.2007.00673.x>.

Szalai, S., Szarka, L., 2008b. Parameter sensitivity maps of surface geoelectric arrays, I. Linear arrays. *Acta Geod. Geophys. Hung.* 43 (4), 419–437. <http://dx.doi.org/10.1556/AGeod.43.2008.4.4>.

- Szalai, S., Szarka, L., 2008c. Parameter sensitivity maps of surface geoelectric arrays, II. Nonlinear and focussed arrays. *Acta Geodaet. Geophys. Hung.* 43 (4), 439–447. <http://dx.doi.org/10.1556/AGeod.43.2008.4.5>.
- Szalai, S., Szarka, L., Prácer, E., Bosch, F., Müller, I., Turberg, P., 2002. Geoelectric mapping of near-surface karstic fractures by using null-arrays. *Geophysics* 67, 1769–1778.
- Szalai, S., Szarka, L., Marquis, G., Sailhac, P., Kaikkonen, P., Lahti, I., 2004. Collinear null arrays in geoelectrics. *Proceedings of the 17th EM Induction Workshop: Hyderabad, India*, 18–23 October, 2004, S.3–P.3 IAGA WG 1.2.
- Szalai, S., Novák, A., Szarka, L., 2009. Depth of investigation and vertical resolution of surface geoelectric arrays. *J. Eng. Environ. Geophys.* 14, 15–23.
- Szalai, S., Novák, A., Szarka, L., 2011. Which geoelectric array sees the deepest in a noisy environment? Depth of detectability values of multielectrode systems for various two-dimensional models. *Phys. Chem. Earth* 36, 1398–1404.
- Szalai, S., Koppán, A., Szokoli, K., Szarka, L., 2013. Geoelectric imaging properties of traditional arrays and of the optimized Stummer configuration. *Near Surf. Geophys.* 11, 51–62.
- Szalai, S., Kis, Á., Metwaly, M., Lemperger, I., Szokoli, K., 2014. Increasing the effectiveness of electrical resistivity tomography using γ_{11n} arrays. *Geophys. Prospect.*
- Wilkinson, P.B., Meldrum, P.I., Chambers, J.E., Kuras, O., Ogilvy, R.D., 2006. Improved strategies for the automatic selection of optimised sets of electrical resistivity tomography measurement configurations. *Geophys. J. Int.* 1119–1126.